Methane activation by CoO_m^{n+} (n = 0, 1, 2; m= 1, 2): reactivity parameters, electronic properties and binding energy analysis

Telles Cardoso Silva, [a,b] Maíra dos Santos Pires, [a] Alexandre Alves de Castro, [a] Lívia Clara Tavares Lacerda, [a] Marcus Vinícius Juliaci Rocha, [a] Teodorico C. Ramalho. [a]

[a] Department of Chemistry. Federal University of Lavras, University Campus, 37200-000, Lavras-MG, Brazil.

[b] Federal Center of Technological Education of Minas Gerais - Varginha Unit, Av Immigrants, 1000, 37022-560, Varginha - MG, Brazil.

Abstract

The need for renewal, more efficient and conscious usage of energy resources has led to a great interest in carrying out studies aiming to find novel sources of energy, which are able to supply the growing global demand, and at the same time, providing an eco-friendly usage of natural resources. In this context, the usage of methane stands out as a promising energetic alternative for this goal, mostly due to the existence of vast reserves, its low cost and less polluting fuel. For theoretical calculations B3LYP, CCSD (t) and ZORA-B3LYP methods were used to look into the catalytic properties of (CoO_m^{n+} n= 0, 1, 2 and m=1, 2) in the methane C-H bond activation. According to the EDA outcomes, the studied species presented two stabilizing factors for the global interaction energy, being the electrostatic ΔE_{elstat} and orbital ΔE_{orb} interactions. The HOMO and LUMO orbitals were also evaluated based on the molecular orbital diagrams for the monoxides and dioxides series. Regarding the oxidative insertion mechanism, the outcomes demonstrate that the initial interaction between oxide and methane is of great relevance in its activation process, in which $E_{Bonding}$ is benefited by the increasingly charge on the central metal. The high electron density regarding the oxides is meaningful for the reaction kinetics and the oxo ligands influence the thermodynamics of the reaction, becoming the DHA mechanism exergonic. Regarding the OHM mechanism, better kinetic conditions are found for CoO_2^{++} and better thermodynamics for doubly charged cobalt monoxides and dioxides.

Keywords

Methane . C–H bond activation . Cobalt oxides . Theoretical study . Gas phase

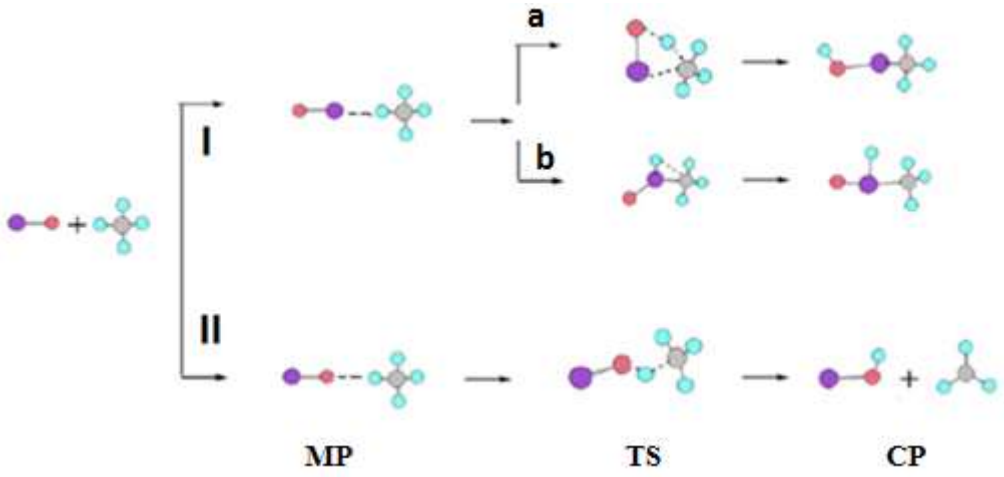

Figure 1. Scheme of molecular structures of the MP, TS and CP complexes for the 4-center hydrogen abstraction mechanism (Ia), oxidative insertion mechanism (Ib) and direct hydrogen abstraction mechanism (II).

INTRODUCTION

The growing overall need for energy brought about by the technological development of society has led to the development of researches aiming at safer and more economical energy sources.[1-5] Natural gas (NG) appears as a promising alternative resource for energy supply owing to the discovery of vast reserves, low cost and by being a less polluting fuel and source of raw material and fuel generation for modern industry. [5, 6-9]

The NG, constituted by 80-90% methane,[7, 10-11] is available worldwide.[5, 9,10] Most of its reserves are found in distant areas that are difficult to access; thus, transport and storage are inconvenient and not feasible in economic terms, due to the high energy costs in the methane transformation to fine commodities.[12,13]

In this way, the major challenge facing the chemical industry is how to activate methane in an economical and clean way, causing less damage to the environment.[14] In this context, several works have been accomplished aiming at more effective catalysts of transition metals that could activate the C-H bond in an efficient and selective way, thus making possible its large-scale application. [6, 10, 12, 15-23] The efficiency of the transformation reaction concerning the conversion of methane to methanol and the branching ratio of methanol are significantly based on the transition metals.[24,25]

The methane activation (gas phase) by first-line transition oxide ions (MO), wherein M being Sc, Ti, V, Cr, Mn, Fe, Co, Ni and Cu is proposed to proceed in two steps by means of two transition states.[17-19,24,26,27] Regarding the first-line metals, the CoO^+ ion displays a high branching ratio for methanol and its high rotation and low rotation potential energy surfaces (PESs) intercept twice in the input channel of the reaction, along with the output channel.[19,24,25] Based on the work from CHEN et al., the mechanism involved in the process of methane conversion to gas phase methanol by cobalt monoxide produces an intermediate HO-Co-CH_3, which is quite important for this reaction.[28]

Cobalt oxides are species that have been considered promising for an efficient transformation process of methane to methanol.[24,25,28] Due to this feature and other factors, several experimental and theoretical works have been conducted with the goal of analyzing the properties of this oxide in the methane C-H bond activation. [25, 29-32] In the work from Bitler et al., the authors studied the C-H bond activation by cobalt-doped ZSM-5 zeolite.[33] In their study, 1.2 μmol of methanol/g of catalyst was produced with a selectivity of about 75%.[33]

In line with this expectation, more information can be extracted by looking into reactivity parameters, electronic properties and binding energy analysis of CoO_m^{n+} (n = 0, 1, 2; m=1, 2). Thus, our main goal was to perform a detailed study by employing computational methodologies of quantum calculations on each aspect of the gas-phase methane activation reactions by cobalt oxides CoO_m^{n+} (n = 0, 1, 2; m=1, 2). This kind of analysis is quite relevant and required. This theoretical procedure provides a viable route for applications, in economic terms, but also opens a new standpoint to study new options for obtaining catalysts with a more promising and rich electronic structure, presenting great scientific, environmental and economic importance.

COMPUTATIONAL DETAILS

The first methods were conducted in order to look into diverse properties of Cobalt oxides (CoO_m^{n+} n= 0, 1, 2 and m=1, 2), in terms of geometric and electronic features. For this analysis, the electronic states regarding Co (doublet, quartet and sextet), Co^+ (singlet, triplet, quintet) and Co^{2+} (doublet, quartet and sextet) were considered with the goal of analyzing the energy difference among the different multiplicities, and also to investigate the relevance of the spin crossings within the

reaction pathways; a characteristic commonly referred to as reactivity of two states [17,26,27] For the accomplishment of these calculations, we employed the Gaussian. 2009 computational package [34] and all calculations were performed considering a gas phase environment.

In the first stage of the work, geometry optimization calculations and frequency analysis were carried out using different computational methods.[35] The methods employed were DFT (Density Functional Theory) and Coupled Cluster (CCSD (T))[35,36]. Regarding the DFT method, it was used in this computational simulation the B3LYP three-parameter hybrid functional which was successfully employed previously, in works involving transition metals species.[37-41] These techniques are mentioned as B3LYP hereafter. In these calculations, the WATCHERS f base sets were employed for the Cobalt atom, [42] while an extended polarized basis assembly, called 6-311G++(d,p)[43] was employed for the Oxygen atom.

A comparison of the B3LYP outcomes for cobalt oxides with data acquired from the CCSD (T) calculations is presented in the supplementary information. The single point CCSD (T) calculations with the cited atomic base sets were performed with the purpose of ensuring high quality levels regarding the energy differences, for which corrections regarding zero-order energy were also considered, at the B3LYP level.

In these calculations, no restriction of symmetry was imposed during geometry optimizations. The vibrational analyzes were performed with the purpose of verifying the character (minimum point or saddle) of all stationary points, and the corrections from the B3LYP zero-point energy (ZPE) method were important in all relative energies.

Secondly, zero-order regular approximation (ZORA)[44] calculations were carried out by employing the ADF2009 software package.[45,46a,b] The functional applied was BLYP, [35] the basis set used was of the polarized triple-zeta Slater type (TZ2P) for the iron and oxygen atoms. [47,48]

With the determination of the optimized geometries of cobalt oxides, we set out to investigate their geometrical and electronic properties and the analysis of the bonds to obtain detailed data from the atomic and molecular standpoint of the characteristics of the chemical bonds of these oxides under study.

The analyzes of the bonds were made by using AIM calculations with the aim of determining the covalent or ionic character of the bonds. The properties related to the electron density regarding the CoO chemical interactions were investigated by

employing atoms in molecules (AIM) theory by Bader, which is implemented in the AIM2000 program.[49] The AIM parameters found at the bond critical points (BCP) are meaningful tools for the description of chemical bonds. [49]

Along with the AIM calculations, and in order to study the participation of the orbitals and the energies concerning the appearing of the chemical bonds in the oxides, it was performed an Energy Decomposition Analysis (EDA), proposed by Morokuma[50] and Ziegler and Rauk. [51] All binding analyzes were performed at the ZORA-BLYP / TZ2P computational level. [47,48] In the EDA calculations, the general bond energy ΔE between the cobalt atom (Co) and the oxygen atoms (O) is constituted by two principal components, equation 1. [52]

$$\Delta E = \Delta E_{Prep} + \Delta E_{int} \quad (1)$$

It is fundamental to notice that from EDA, there is the decomposition of the instantaneous interaction energy E_{int} between two portions A and B in a molecule A-B, in three terms that are well-defined (equation 2), they are: the energy regarding the quasiclassic electrostatic interaction among the charge densities of the portions (ΔE_{elstat}), the exchange repulsion among the parts due to the Pauli principle (ΔE_{Pauli}) and the energy gain from the orbital mixture of the portions (ΔE_{orb}). The orbital interaction ΔE_{orb} in the Kohn-Sham theory explains the charge transfer (i.e., donor-receiver interactions between occupied orbitals in a portion and unoccupied ones on the other, including HOMO-LUMO interactions) and polarization (empty / occupied orbitals mixture in a portion, due to the presence of a second one).

$$\Delta Eint = \Delta E_{elstat} + \Delta E_{Pauli} + \Delta E_{orb} \quad (2)$$

The deformation energy ΔE_{Prep} or $\Delta_{Estrain}$ is the amount of energy needed to deform the Co and O fragments.

The reaction mechanisms which are experimentally recognized to activate the C-H chemical bonds by the performance of transition metal oxides have been evaluated. In this part of the study, the kinetic and thermodynamic preference of different products from the reaction of interest was analyzed in detail. In this investigation, the molecular complexes regarding the methane C-H bond activation were verified, e.g., molecular

precursor (MP), transition state (TS) and complex product (CP) for the entire series of cobalt oxides under investigation.

To guarantee the correct reaction, the path of the lower energy structures of two intermediate consecutive periods, intrinsic reaction coordinate (IRC) calculations were carried out [53], which are performed to correctly optimize the TS linking the intermediates under investigation.[18, 43, 54] The vibration analyzes were then accomplished to look into the character concerning stationary points (minimum or saddle point). We are able to ensure this, since each TS structure obtained in PESs shows only one imaginary frequency, which correctly drives to the correct intermediate.

Results and discussions

This work is an important starting point, which can lead us to a better understanding in what concerns the electronic structures of the CoO_m^{n+} (n = 0, 1, 2; m=1, 2) prototypes. The obtained results might provide us relevant information, assisting in the search for more effective catalysts, which react under mild conditions, of sustainable and clean way.

In these studies, the first step is the verification of the geometric, electronic and binding properties of cobalt oxides. In Table SI-1, experimental and computed geometrical properties as well as the multiplicity for cobalt oxides are described. After these calculations, electronic and binding properties were analyzed and described in the first section of this article.

Study of the electronic and binding properties of CoO_m^{n+} (n = 0, 1, 2; m=1, 2)

For a quantitative and qualitative interpretation of the chemical bonds nature of cobalt oxides, an energy decomposition analysis (EDA), developed by Morukuma[50] and by Ziegler and Rauk[51] was employed. From EDA, the interaction energy of cobalt with the oxygens is decomposed in three terms defined to ΔE_{Pauli}, ΔE_{elstat} and ΔE_{orb}, providing a chemically significant interpretation of chemical bonds. [55, 56]

Table 1 shows the outcomes from the EDA analyzes of the cobalt oxide prototypes. For the acquirement of more accurate data, we employed the BLYP functional, which besides correcting the influence of the dispersion interactions in the

results, it is worth mentioning that this functional is broadly used for calculations involving transition metals. [57]

Table 1. Energy Decomposition Analysis of the CoO_m^{n+} (n = 0, 1, 2; m=1, 2) at ZORA BLYP/TZ2P, in kcal.mol^{-1}

Oxides	CoO	CoO^+	CoO^{++}	CoO_2	CoO_2^+	CoO_2^{++}
ΔE_{Pauli}	0.52	0.51	0.30	0.53	0.52	0.28
ΔE_{elstat}	-1.49	-2.05	-2.37	-1.33	-1.84	-2.15
ΔE_{orb}	-0.56	-0.99	-1.77	-0.58	-1.00	-1.80
ΔE_{int}	-1.54	-2.53	-3.84	-1.39	-2.32	-3.66

According to the calculations, given that there is no geometric and electronic preparation of the atomic fragments Co and O at $\Delta E_{prep} = 0$, the interaction energy is similar to the binding energy for CoO_m^{n+} (n = 0, 1, 2; m = 1, 2). Thus, the EDA outcomes indicated that the species under investigation have two stabilizing factors to the global interaction energy, i.e., the electrostatic ΔE_{elstat} and orbital ΔE_{orb} interactions. As there were no positive values for ΔE_{orb}, configurations of the Co and O fragments are likely correct. The Pauli repulsion results are positive owing to some interactions among the occupied orbitals (destabilizing ones) in the fragments, and they account for the effects of steric repulsion among the portions. Those ΔE_{Pauli} values decrease along the oxides series.

The values of the term ΔE_{Elstat} decrease throughout the monoxides and dioxides series, ranging from -1.49 to -2.37 kcal/mol regarding the monoxides, and from -1.33 to -2.15 kcal/mol regarding the dioxides. One can realize a larger contribution of this term for the monoxides in relation to the dioxides, which comes from a stronger interaction of the core of the cobalt atoms that carry a positive charge and an oxo ligand that carries a much greater negative charge than the dioxides. Another fact that proves this growth of ΔE_{Elstat} is the augmentation of electron density for the monoxides according to table 2, regarding the QTAIM results.

Considering the monoxides series, CoO^{++} presents the highest stabilizing contributions to the global interaction energy, which are ΔE_{elstat} with a value of -2.37 kcal/mol and ΔE_{orb} with a contribution of -1.77 kcal/mol. Differently, CoO presents a higher positive value of ΔE_{Pauli} throughout the series, with a value of 0.30 kcal/mol.

This outcome comes from greater interaction between the cobalt and oxygen atoms coming from the smaller size of the oxide, which causes a larger repulsion of their spins with the same rotation.

The EDA outcomes for the dioxides series follow the trend of the monoxides series, with a lower electrostatic contribution owing to the reduction of the electron density (table 2), and a larger contribution of ΔE_{orb} due to the orbital interaction of the cobalt with two oxygens. Among the dioxides series, CoO_2^{++} presents the highest stabilizing contributions, ΔE_{elstat} with a value of -2.15 kcal/mol and ΔE_{orb} with a contribution of -1.80 kcal/mol.

Comparison of the cobalt monoxide and dioxide series shows that a detailed analysis of all individual terms of the global interaction energy is needed to understand the strength and nature of a chemical bond. The EDA outcomes indicated that the stabilizing energies ΔE_{elstat} and ΔE_{orb} favored the higher global interaction energies of the monoxides and divalent dioxides, corroborating with the work from Spackman, [58] whose work demonstrated that electrostatic interactions are very important for chemical bonds in almost all molecules. Regarding the cobalt prototype series, the monoxides showed a larger ΔE_{int} owing to a higher electron density in relation to the dioxides, and also by the polarity of the bond that favored the ΔE_{elstat} stabilization.

Figure 2 presents the orbital correlation diagram illustrating the orbitals involved in the interactions of a d^6 transition metal with oxygen. Table SI-1, supporting information, reports the contribution percentages of the orbital fragments of C_1 symmetry cobalt oxides to monoxides and D_2H to dioxides implicated in the formation of highest occupied molecular orbitals, denominated HOMO, along with the formation of the lowest unoccupied molecular orbitals, LUMO.

It is relevant to mention that, according to table SI-1, the LUMO orbitals consist of a large contribution of the d and s orbitals of the metal and a smaller percentage of the p orbital of the oxygen. The mono and divalent monoxides and dioxides present a greater participation of the dz^2 orbital. This contribution increases throughout the monoxides and dioxides cobalt series owing to the removal of the electrons from this orbital, because of the increased charge of the metal. Regarding the doubly degenerate (d2g) HOMO orbitals, the major contributions concern the d_{xy} and $d_{x^2-y^2}$ orbitals of cobalt. According to the results from table SI-1 arranged in the support information, cobalt is involved in donation and receipt of electrons.

It is necessary to comment that molecular orbitals are significant descriptors for the rationalization of diverse reactions, and present a special importance in the understanding of chemical reactivity. [17, 59] Thus, Figure 2 exhibits a parallel between the HOMOs and LUMOs of the cobalt prototypes under study. With the augmentation in the cobalt charge over the cobalt monoxides and dioxides series, there is a decrease in the HOMO and LUMO energies. For example, HOMO orbitals for monoxides range from -0.24 to -0.89 eV and the LUMOs orbitals -0.08 to -0.79 eV. Thus, it is easy to realize that the HOMO - LUMO energy differences are related to the fluctuation of the electron density, along with the polarity of the Co-O bond.

The orbitals diagram, Figure 2, demonstrates that the electrons less attached to the bond are the σ_{Co-O} of the neutral monoxides and dioxides. Thus, it is easy to realize that CoO and CoO_2 are considered the best σ electron donors. This factor can be comprehended by the higher electron density of these oxides obtained by the QTAIM calculations. On the contrary, Figure 2 indicates that the best electron acceptors, the empty orbital of lower energy, are the σ^*_{Co-O} of the divalent monoxides and dioxides. This characteristic comes from the higher participation of the unoccupied $3dz^2$ orbital of cobalt, and owing to the lower electron density of these oxides (Table 3). [60]

The EDA results show the relevance of their association with the outcomes from the QTAIM calculations for understanding the nature of the chemical bond (e.g., whether the bond is covalent, partially covalent or non-covalent).

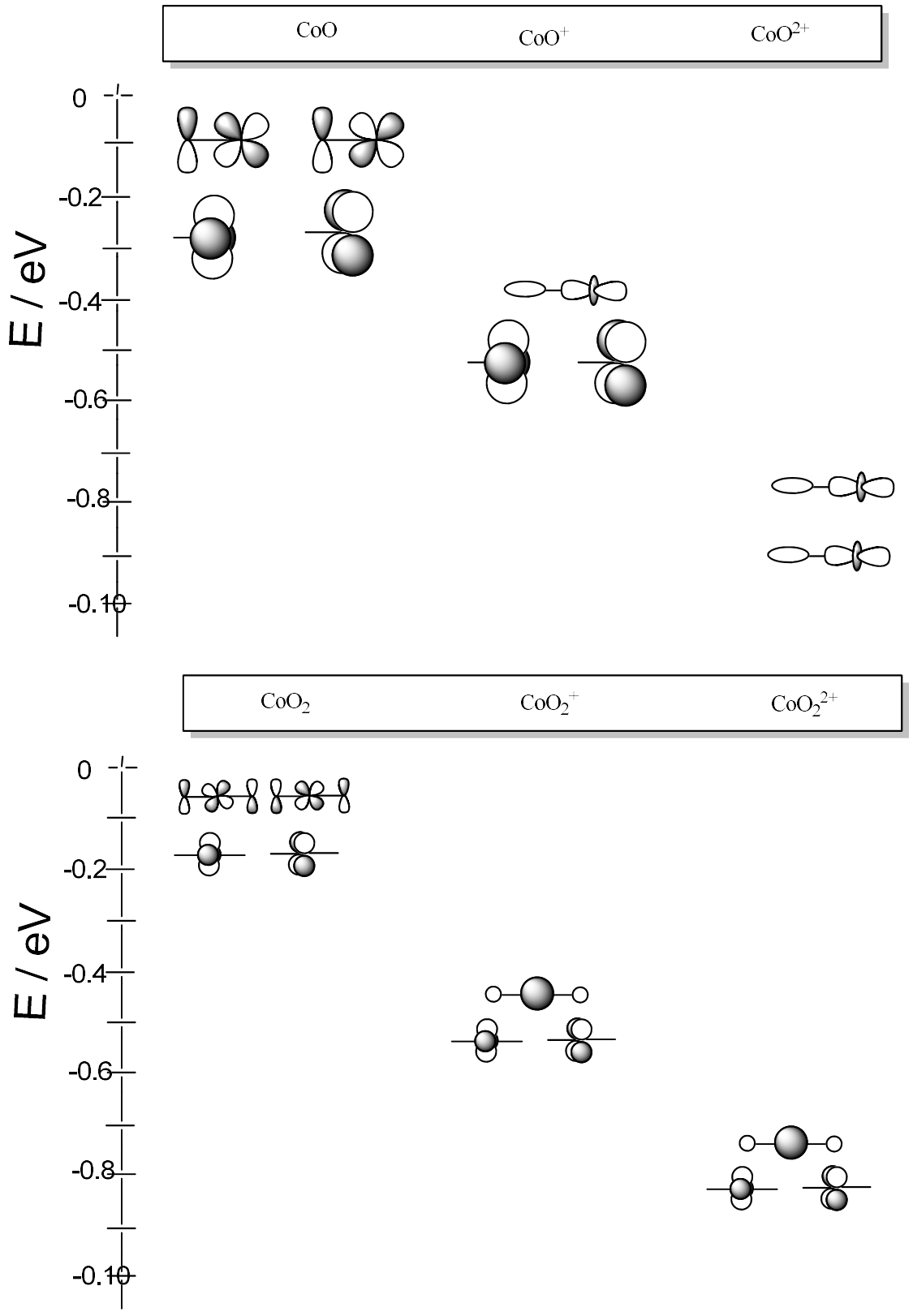

Figure 2. Diagram of the HOMO and LUMO molecular orbitals for cobalt oxide prototypes, emerging from Kohn-Sham orbital analyzes in ZORA-BLYP / TZ2P.

AIM Analyses

Table 2 contains all the parameters of the cobalt oxides prototypes resulting from the AIM calculations. According to the calculations, the point where the charge density function (q (r)) is a minimum along the binding path and maximum in the other two directions, i.e., the bond critical point (BCP) is located at center of the Co-O bond of all cobalt oxide prototypes.

TABLE 2: The AIM B3LYP/ Watchers f parameters, electron density (p(r)), Laplacian ($\nabla^2 p$(r), total electron energy density (H(r)), kinetic electron energy density (G(r)), and potential electron energy density (V (r)) for bcp of the Co-O chemical bonds of the ground-state cobalt prototypes. **

Species	p(r) (a.u)	$\nabla^2 p$(r) (a.u)	G(r) (a.u)	V (r) (a.u)	-G/V	H (r)
CoO	+0.2056	+0.9415	+0.3319	-0.4284	0.7747	-0.0965
CoO^+	+0.1867	+1.0260	+0.3342	-0.4119	0.8113	-0.0777
CoO^{2+}	+0.0886	+0.4012	+0.1090	-0.1178	0.9252	-0.0088
CoO_2	+0.1906	+1.0725	+0.3512	-0.4343	0.8086	-0.0831
CoO_2^+	+0.1671	+0.9871	+0.3071	-0.3674	0.7071	-0.0603
CoO_2^{2+}	+0.1284	+0.7238	+0.2106	-0.2403	0.8764	-0.0297

**Computed outcomes were performed by employing the AIM program.

According to the results in Table 2, the values computed for p(r) at the critical point of the Co-O bond decrease along the cobalt oxides series, ranging from +0.2056 a.u. to +0.0886 a.u. for the monoxides and +0.1906 a.u. to +0.1284 a.u. for the dioxides. These outcomes suggest that the higher p(r) values are calculated for the neutral cobalt oxides, and that the value of this parameter decreases with increasing load on the metal center. Therefore, these p(r) results confirm our interpretation of the EDA, in which they indicate more favorable interaction energy for the monoxides and divalent dioxides.

All Co-O bonds have positive values for ∇^2p(r) (a.u.), suggesting that the atomic nuclei support the entire charge concentration and that the electron density is accumulated on cobalt. To verify the nature of the Co-O bond, it is necessary the study of some parameters, such as ∇^2p(r), -G/V and H (r). It is possible to interpret according to Table 2 that, although ∇^2p(r) has positive values indicating an ionic character, the Co-O bond also presents a partial covalent character, due to the other parameters -G/V> 0

and H (r) <0. Therefore, one can observe that the AIM calculations outcomes indicate that the Co-O chemical bonds have a partial ionic and covalent character.

After the studies with the cobalt oxides, in terms of electronic and binding properties, the next step was to analyze the activation mechanisms of the methane C-H bond. To date, no cobalt oxide series investigations have been found in this activation process. Such analyzes are reported in the second section of this article.

The Methane C-H bond Activation Process.

Cobalt oxides have been drawing the attention of the scientific community as a catalyst in inert hydrocarbon reactions owing to its appropriate electronic configuration to activate methane along with the high branching index of methanol in the reaction.

Due to these and other properties, three experimentally recognized mechanisms that concern the activation of the C-H bond were studied in the second part of this work.[13, 20] The first route is the oxidative insertion mechanism (OIM) of a metal center to the methane C-H bond. [13, 61] The second is the C-H bond metathesis by the oxygen of cobalt oxides, called direct abstraction, [62, 63] and the third one, 4-center hydrogen abstraction or oxidative hydrogen migration (OHM), accounted for the formation of the hydroxymethyl intermediate that was produced in a laser ablation source and characterized by electronic and vibrational spectroscopy, in the work from Altinay et al. [19, 25]

All stationary molecular systems related to these reaction mechanisms were investigated in detail. The first system, molecular precursor (MP), which is a weakly bound complex originated in the reaction input channel, had all possible H-type molecular interactions considered, as can be observed in Fig. 3. These conformations, called η^1, η^2 and η^3 showed three different metal interactions with methane. In this step, it was also considered all these options with an oxygen atom from the oxo ligands primarily directed to a specific hydrogen atom of methane.

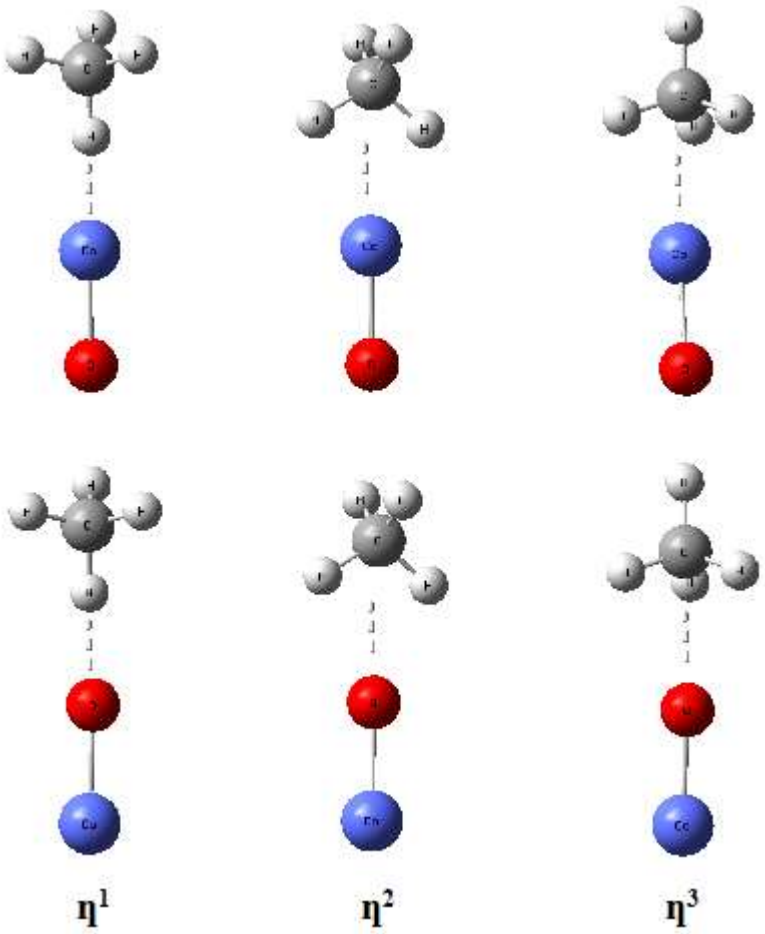

Figure 3. The coordination types of the weakly bound MP *n*-complexes.

Posteriorly to these outcomes, all likely TS organometallic complexes were considered and the optimized conformation drives to the first stable organometallic complexes recognized as complex products (CP). The optimized molecular structures implicated in the reaction mechanisms, MP, TS and CP, were identified by harmonic vibrational frequency such as minimum conformation or transition state.

Oxidative insertion mechanism (OIM)

This mechanism is typical of electron-rich complexes, of the "late" transition metals such as Iron and Cobalt. [13]

In Figure 4, the geometries of the optimized molecules concerning the methane activation process are represented by the OIM.

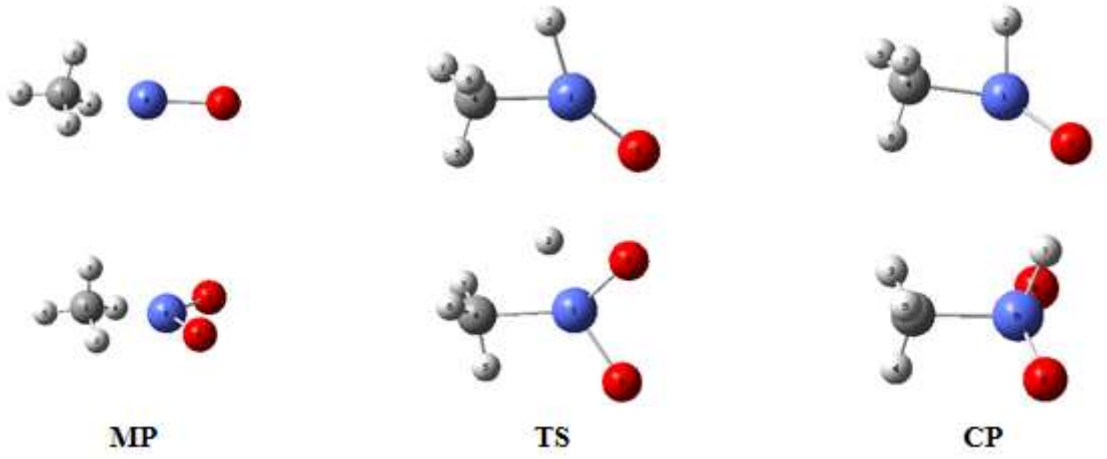

Figure 4. Representation of optimized molecular geometries at the B3LYP level (lowest-energy spin state MP, TS and CP complexes) regarding the OIM.

Based on our outcomes, MP complexes generated by the coordination among methane and metal center presented a preferential conformation η^3 with the cobalt atom directed to the three hydrogen atoms present in methane (figure 4).

By analyzing the factors related to geometry in table SIII-1, a reduction in the Co-C binding lengths along the MP complexes for both monoxides and dioxides is observed. This variation in the Co-C bond length comes from the reduction of electron density regarding the cobalt oxides throughout the series.

CoO and CoO_2 present a higher electron density and these oxides donate this density to the σ^* C-H orbital of methane, resulting in higher Co-C lengths. [64] Since the other oxides of the series have a lower electron density and therefore, the complexes are generated from the electron density interaction (methane σ C-H bond) with the empty d orbital of cobalt. [64] These results corroborate with the EDA and QTAIM.

Comparing the Co-C bond lengths of the monoxides regarding the dioxides, it is easy to notice that the Co-C chemical distances in the MP dioxide complexes are smaller regarding the monoxides, showing that the presence of two oxo ligands and the lower electron density of the dioxide favor the interaction between both species, the metal center and methane (electrostatic), more specifically at the beginning of the reaction.

The TS and CP geometries from the cobalt oxide prototypes after optimization presented a preferential trans conformation that is stabilized regarding the Co-H bonds.

Considering the optimized bond lengths in relation to the TS and CP complexes, a decrease of the Co-C bond lengths along the series for these complexes is observed. This feature indicates a greater interaction between cobalt and methane, conducting the formation of organometallic complexes owing to the introduction of a metal center on the C-H bond.

Concerning the Co-H bond lengths, lower values are observed for the dioxide complexes regarding the monoxides. A smaller difference is noticed for the Co-H bond lengths for the CP complexes in comparison to the TS complexes values.

The computational outcomes of the binding energies, activation energy and reaction energy of the OIM of the species investigated in this work are shown in Table 3.

TABLE 3: Bonding ($\Delta E_{Bonding}$), activation barriers ($\Delta E_{Activation}$) and reaction energies ($\Delta E_{Reaction}$) for the OIM with niobium oxides into the methane C-H bond.*

	$E_{Bonding}$	$E_{Activation}$	$E_{Reaction}$
z	B3LYP	B3LYP	B3LYP
CoO	-12.55	18.82	-12.55
CoO^+	-25.10	69.02	-50.20
CoO^{2+}	-87.85	119.23	-81.57
CoO_2	-18.82	12.55	-31.37
CoO_2^+	-69.03	56.47	-69.02
CoO_2^{2+}	-106.67	81.57	-75.30

*Energies in kcal/mol

By observing the results of the binding energies of the cobalt complexes for the OIM, such energies ranged from -12.55 kcal/mol to -87.85 kcal/mol for the monoxides and from -18.82 kcal/mol to -106.67 kcal/mol for the dioxides. Based on these outcomes, it is worth highlighting that the origin of the electrostatically bonded MP complex is benefited by the decrease in the electron density of cobalt oxides, and the oxo ligands provides an initial electrostatic interaction more favorable for methane, providing an extra dipole interaction.

Regarding the kinetic data of the analyzed mechanism, lower values were found for neutral monoxides and dioxides, and the dioxides presented lower energy barriers in

comparison to the cobalt monoxides. We can, thus, conclude that this result comes from the low electron density of the participating dioxides in the formation of TS organometallic complexes.

The balance which can be observed between kinetic and thermodynamic factors will determine whether the process concerning the methane activation is going to take place. In face of this consideration, it is noteworthy the fact that gas phase reactions are supposed to occur if all stationary points are located below the reactive energies.

According to the results displayed in Table 3, the OIM of cobalt with methane are all exergonic. It is presented that the thermodynamics regarding this process is favorable with increasing load on the metal center, and also with increasing the oxo ligands. The ratio of these outcomes can be correlated with the electronic configurations of Co, Co^{+} and Co^{2+} species, which are [Ar] $3d^6 4s^2$, [Ar] $3d^6 4s^1$ and [Ar] $3d^6$, respectively. In the production of CP organometallic complexes, it is required an electronic configuration capable of making two covalent bonds, Co-H and Co-CH_3 for their formation.

Hydrogen abstraction mechanism (HAM)

Other processes concerning the methane activation are the mechanisms of direct hydrogen abstraction (DHA) and 4-center hydrogen abstraction or oxidative hydrogen migration (OHM). The DHA mechanism is a kind of external sphere mechanism, in which involves an abstraction process of the hydrogen from methane directly by the oxygen of the cobalt oxides, leading the origin of the MP complex of η^1 conformation, [18] according to Figure 5.

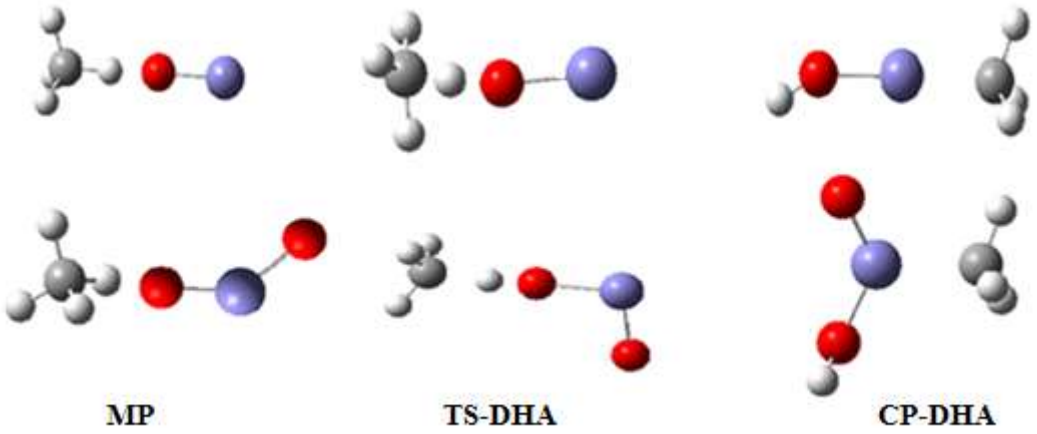

Figure 5. Representation of optimized molecular geometries at the B3LYP level (lowest-energy spin state MP, TS and CP complexes) regarding the DHA.

The OHM takes place by means of an internal sphere mechanism, in which the metal interacts directly with the methane C-H bond. [17, 18, 61] In the mechanism exposed in Figure 6, at the entrance channel of the reaction, the production of a complex of η^3 conformation occurs, in which the cobalt oxides point directly to the three hydrogens of methane. Throughout the reaction, there is the generation of a 4-centered transition state, which leads to an intermediate reaction involving the ligands OH and CH_3 (OH-Co-CH_3), without the formation of an alkyl radical in the course of the reaction.

In the three mechanisms studied, only the stage of formation of MP, TS and CP, limiting step of the alteration of methane to methanol called C-H bond activation, was verified in this work.

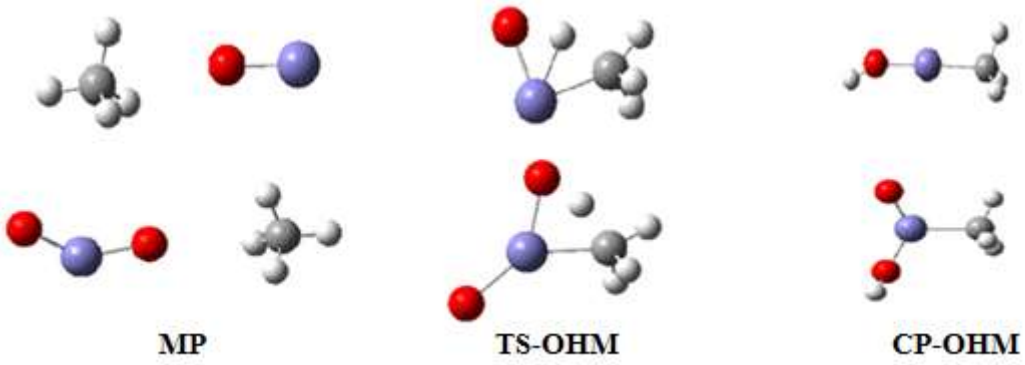

Figure 6. Representation of optimized molecular geometries at the B3LYP level (lowest-energy spin state MP, TS and CP complexes) regarding the 4-OHM mechanism.

According to Figure 5 and 6, it is easy to observe the distinctions between the abstraction mechanisms, because in the OHM mechanism, there is a relevant interaction between the cobalt and the active center of the carbon atom of the substrate, forming the hydroxymethyl organometallic complex.

In Table SIII-2 and 3, the parameters related to geometry regarding binding lengths and binding angles for the DHA and OHM mechanisms are shown.

Regarding the values of these parameters in relation to the cobalt complexes in the direct abstraction mechanism, presented in the support information, a decreasing behavior of the O-H bond lengths throughout the series for both monoxides and dioxides is observed. The cobalt dioxides have lower values indicating a more efficient interaction because of the presence of the second oxygen in comparison to the monoxides.

For the 4-center abstraction mechanism, there is a reduction in the length of the Co-C bond in the oxide series for all complexes formed indicating once more the strong interaction of cobalt oxides with methane to form stable complexes. An inverse trend has been noticed for the Co-O bond lengths which indicates that this bond length of the oxides becomes weaker with coordination with methane. In particular, this characteristic is highlighted as the amount of increases of oxo ligands.

The thermodynamic and kinetic results of the HAMs are shown in Tables 4 and 5.

TABLE 4: Bonding ($\Delta E_{Bonding}$), activation barriers ($\Delta E_{Activation}$) and reaction energies ($\Delta E_{Reaction}$) for the direct abstraction with cobalt oxides into the methane C-H bond.*

	$E_{Bonding}$	$E_{Activation}$	$E_{Reaction}$
Species	B3LYP	B3LYP	B3LYP
CoO	-12.55	14.27	9.41
CoO^+	-25.10	16.55	11.27
CoO^{2+}	-100.40	18.82	-50.20
CoO_2	-25.10	19.41	-25.10
CoO_2^+	-100.4	26.1	-51.57
CoO_2^{2+}	-106.77	16.87	-53.92

*Energies in kcal/mol

TABLE 5: Bonding ($\Delta E_{Bonding}$), activation barriers ($\Delta E_{Activation}$) and reaction energies ($\Delta E_{Reaction}$) for the 4-center abstraction with cobalt oxides into the methane C-H bond.*

	$E_{Bonding}$	$E_{Activation}$	$E_{Reaction}$
Species	B3LYP	B3LYP	B3LYP
CoO	-12.55	31.37	-56.47
CoO^+	-25.10	34.51	-62.75
CoO^{2+}	-87.85	43.92	-94.12
CoO_2	-18.82	56.47	-69.02
CoO_2^+	-69.03	25.10	-87.85
CoO_2^{2+}	-106.67	12.55	-144.32

*Energies in kcal/mol

The $E_{Bonding}$ values for the abstraction mechanisms decrease throughout the cobalt monoxides and dioxides series suggesting that the initial interaction between these oxides and methane is benefited by the production of the MP complexes. These computed outcomes might indicate that the increased oxo ligands in coordination to the metal center are essential at the beginning of the entrance channel of these gas phase

reactions. This can be explained by the electron accepting characteristic of these oxides, as described in the QTAIM results.

The activation energies values of the DHA mechanism increase with load on the metal center and by adding the second oxo ligand, with the exception of CoO_2^{++}. This trend follows for the OHM mechanisms concerning the cobalt monoxides and, regarding the dioxides, an opposite trend is observed. This result indicates that oxo ligands are important in the OHM-TS formation.

The activation barrier regarding the DHA mechanism ranges from 14.27 to 18.82 kcal/mol for the monoxides and from 19.41 to 16.87 kcal/mol for the dioxide series, by one hand decreasing the activation barrier, and by the other hand increasing the kinetics of the reaction. For the 4-center abstraction mechanism, the values range from 31.37 to 43.92 kcal/mol for the monoxide series, and from 56.47 to 12.55 kcal/mol for the dioxide series.

General results for the DHA mechanism indicate better kinetic conditions and thermodynamics for the doubly charged cobalt dioxides. According to these outcomes, it is possible to realize that oxo ligands influence the thermodynamics of the reaction, making the DHA mechanism exergonic.

Concerning the OHM mechanism, better kinetic conditions are found for CoO_2^{++} and better thermodynamics for doubly charged cobalt monoxides and dioxides. According to these findings, it is given that a low electron density of oxides and oxo ligands are important for kinetics and thermodynamics of the reaction.

Finally, the best outcomes obtained for the 4-center abstraction mechanism were for the divalent cobalt dioxide due to high-spin states and spins crossing between the quartet and sextet multiplicities in the input channel and at the end of the reaction.

Figure 7 displays the PES for the OHM reaction of CoO_2^{++} by employing the B3LYP/Watchers method. Based on the figure, the pathway which presents minimum energy firstly involves the MP formation. The hydrogen abstraction *via* OHM-TS conducts to the CP intermediate $[HO - Co - CH_3]^{++}$. The reagent CoO^{++} has a ground state of the sextet and throughout the reaction pathway, sextet and quartet change of rotation in the input and output channel of the reaction.

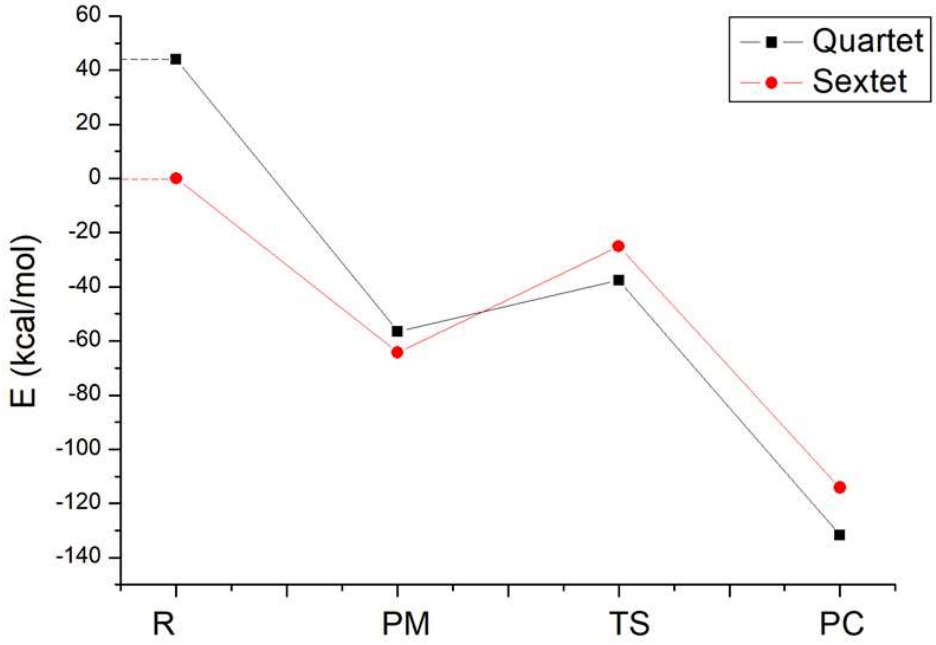

FIGURE 7. PES of the OHM mechanism for the most thermodynamically favorable CoO_2^{++}. Energies (in kJ/mol) have been computed by employing the B3LYP / Watchers theory level.

From the energy values, it is shown that both HAMs can occur in the methane activation, in the gas phase, involving cobalt oxides, but with low efficiency at room temperature. Furthermore, once the insertion intermediate is formed (CH_3-Co-OH), CH_3OH is selectively produced. [25, 28]

Final Considerations

Based on the research results of the geometric and electronic factors of cobalt oxides, it is easy to realize that the monoxides bond lengths are smaller than those of the dioxides. These values concern the highest electron density and electrostatic force between Co and O atoms, which can indicate that the bonds of the monoxides are stronger than the bonds of the dioxides, and all have a partial ionic and covalent character, according to the AIM calculations.

Results from the EDA demonstrated that the compounds under investigation have two stabilizing reinforcements to the total interaction energy, i.e., the electrostatic

ΔE_{elstat} and orbital ΔE_{orb} interactions, with a larger contribution of the term ΔE_{elstat} to the monoxides regarding the dioxides. This contribution comes from a stronger interaction of the nuclei of the cobalt atoms that carry a positive charge and an oxo ligand that carries a much greater negative charge than on the dioxides, and also due to the higher electron density of the monoxides.

According to the molecular orbital diagram, the LUMO orbitals consist of a large contribution of the d and s orbitals of the metal and a lower percentage of the p orbital of the oxygen. Regarding HOMO orbitals doubly degenerate (d2g), the major contributions are related to the d_{xy} and $d_{x^2-y^2}$ orbitals of cobalt and the energies of these orbitals decrease over the cobalt monoxides and dioxide series.

The EDA calculations also showed that CoO and CoO_2 are considered to be the best σ electron donors and that the best electron acceptors, the lowest energy empty orbital, are the $\sigma^*_{Co\text{-}O}$ of the CoO^{2+} and $CoO_2{}^{2+}$.

Concerning the reactivities of cobalt oxide prototypes, for the OIM, our findings demonstrated that the initial interaction between oxide and methane is quite important in the methane activation process, in which $E_{Bonding}$ is benefited by the increased load on the metal center. In addition, it is important to highlight that the oxo ligands lead to an additional electrostatically dipole interaction for methane, and this allows for having an improvement concerning the polarization of this inert molecule at the beginning of the reaction. Another important result is that the kinetics of activation process is not influenced by the presence of oxo ligands. This comes the fact that oxo ligands present good electron acceptor capacity, thus making it difficult to oxidatively add the metal center to the methane C-H bond.

Regarding the HAM, it is interesting to notice differences among the mechanisms studied, because the OHM mechanism shows a meaningful interaction between the cobalt and the active center of the carbon atom of the substrate, resulting in the production of the hydroxymethyl.

General outcomes for the DHA mechanism indicate better kinetics and thermodynamics for doubly charged cobalt dioxides. Based on these findings, we can realize that the oxo ligands influence the thermodynamics of the reaction, making the DHA mechanism exergonic.

Concerning the OHM mechanism, better kinetic conditions are found for $CoO_2{}^{++}$ and better thermodynamics for doubly charged cobalt monoxides and dioxides. Based on these outcomes, we can observe that the low electron density of the oxides and the

oxo ligands are important in what concern the kinetics and thermodynamics of the reaction, and that the OHM mechanism is more propitious than DHA, in thermodynamic terms.

The investigation of catalytic functionalization processes of methane, which are efficient, potentially clean and sustainable, has great scientific importance. Thus, in this study it was possible to obtain a good knowledge about the reactivity, selectivity and electronic structures of the cobalt oxide prototypes, concerning the processes for methane C-H bond activation.

Acknowledgements

The authors wish to thank the Brazilian financial agencies Coordenação de Aperfeiçoamento de Pessoal de Nível Superior (CAPES) for financial support, and the Federal University of Lavras (UFLA) for providing the physical infrastructure and working space. This work was also supported by excellence project FIM and UHHK.

Conflicts of interest

The authors declare that there is no conflict of interests regarding the publication of this paper.

Bibliographical references

[1] International Energy Agency, OECD/IEA, **2017**.

[2] A. A. Castro, I. G. Prandi, K. Kuca, T. C. Ramalho, *Ciênc. e Agrotec.* **2017**, *41*, 471-482.

[3] T. S. Tavares, J. A. Torres, M. C. Silva, F. G. E. Nogueira, A. C. Silva, T. C. Ramalho, *Bioprocess. Biosyst. Eng.* **2018**, *41*, 97-106.

[4] A. I. Nguyen, M. S. Ziegler, P. Oña-Burgos, M, Sturzbecher-Hohne, W. Kim, D. E. Bellone, T. D. Tilley, *J. Am. Chem. Soc.* **2015**, *137*, 12865−12872.

[5] T. M. Gür, *Prog. Energy Combust. Sci.* **2016**, *54*, 1-64.

[6] M. Ravi, M. Ranocchiari, J. A. van Bokhoven, *Angew Chem Int Ed*. **2017**, *56*, 16464-16483.

[7] R. Horn, R. Schlogl, *Catal. Lett.* **2015**, *145*, 23-39.

[8] E. D. Sloan Jr, *Nature*, **2003**, *426*, 353- 359.

[9] E. M. dos Santos, Handbook Gás natural, estratégias para uma energia nova no Brasil, São Paulo: Annablume, Fapesp, Petrobrás, **2002**.

[10] N. J. Gunsalus, A. Koppaka, S. H. Park, S. M. Bischof, B. G. Hashiguchi, R. A. Periana, *Chem. Rev.* **2017**, *117*, 8521-8573.

[11] R. H. Crabtree, *Chem Rev.* **1995**, 95, 987- 1007.

[12] Y. Tsuji, K. Yoshizawa, *J. Phys. Chem. C*, **2018**, *122*, 15359-15381.

[13] J. A. Labinger, J. E. Bercaw, *Nature,* **2002**, *417*, 507-514.

[14] J. Guo , H. Lou, X. Zheng, *J. Nat. Gas Chem.* **2009**, 18, 260-272.

[15] P. G. Lustemberg, R. M. Palomino, R. A. Gutiérrez, D. C. Grinter, M. Vorokhta, Z. Liu, P. J. Ramirez, V. Matolín, M. V. Ganduglia-Pirovano, S. D. Senanayake, *J. Am. Chem. Soc.* **2018**, *140*, 7681-7687.

[16] Z. Sun, O. A. Hull, T. R. Cundari, *Inorg. Chem.* **2018**, *57*, 6807-6815.

[17] T. C. Silva, K. J. de Almeida, M. S. Pires, A. A. Castro, M. A. Gonçalves, E. F. F. da Cunha, T. C. Ramalho, *Reac. Kinet. Mech. Cat.* **2017**, *120*, 195–208.

[18] K. J. de Almeida, T. C. Silva, J. L. Neto, M. V. J. Rocha, T. C. Ramalho, M. N. de Miranda, H. A. Duarte, *J. Organomet. Chem.* **2016**, *802*, 49-59.

[19] J. Roithova, D. Schroder, *Chem. Rev.* **2010**, *110*, 1170-1211.

[20] D. Schröder, H. Schwarz, *PNAS*, **2008**, *105*, 18114-18119.

[21] I. W. Davies, J. Wu, J. F. Marcoux, M. Taylor, D. Hughes, P. J. Reider, R. J. Deeth, *Tetrahedron*, **2001**, *57*, 5061-5066.

[22] C. Hall, R. N. Perutz, *Chem. Rev.* **1996**, *96*, 3125-3146.

[23] A. E. Shilov, G. B. Shul'pin, *Chem. Rev.* **1997**, *97*, 2879-2932.

[24] Y. Shiota, K. Yoshizawa, *J. Am. Chem. Soc.* **2000**, 122, 12317-12326.

[25] G. Altinay, A. Kocak, J. S. Daluz, R. B. Metz, *J. Chem. Phys.* **2011**, *135*, 084311-1 – 084311-10.

[26] C. Li, C. Dinoi, Y. Coppel, M. Etienne, *J. Am. Chem. Soc.* **2015**, *137*, 12450-12453.

[27] H. Schwarz, Handbook Chemistry with Methane: Concepts Rather than Recipes, Angewandte Chemie – International Edition, **2011**, *50*, 10096-10115.

[28] Y, Chen, D. E. Clemmer, P. B. Armentrout, *J. Am. Chem. Soc.* **1994**, *116*, 7815-7826.

[29] S. Hirabayashi, R. Okawa, M. Ichihashi, Y. Kawazoe, T. Kondow, J. Chem. Phys. **2009**, *130*, 164304 – 164304-7.

[30] A. M. L. Oiestad, E. Uggerud, *Chem. Phys.* **2000**, *262*, 169-177.

[31] D. Schroder, H. Schwarz, *Angew. Chem. Int. Ed.* **1995**, *34*, 1973-1995.

[32] V. E. Henrich, P. A. Cox, Handbook The Surface of Metal Oxides; Cambridge University Press: Cambridge, **1994**.

[33] N. V. Beznis, B. M. Weckhuysen, J. H. Bitter, Catal. Lett. **2010**, *136*, 52-56.

[34] D. J. Frisch, M. J. Trucks, G. W. Schlegel, H. B. Scuseria, G. E. Robb, M. A. Cheeseman, J. R. Scalmani, G. Barone, V. Mennucci, B. Petersson, G. A. Nakatsuji, H. Caricato, M. Li, X. Hratchian, H. P. Izmaylov, A. F. Bloino, J. Zheng, G. Sonnenb, (Gaussian, Inc., Wallingford CT), Gaussian 09, **2009**

[35] N. H. Morgon, K. Coutinho, Handbook Métodos de Química Teórica e Modelagem Molecular. São Paulo: Editora Livraria da Física, **2007**

[36] S. Saebo, J. Almlof, *Chem. Phys. Lett.* **1989**, *154*, 83-89.

[37] G. Wang, M. Chen, S. Lai, M. Zhou, *J. Phys. Chem. A*, **2011**, *13*, 9514-9520.

[38] R. P. da Silva, J. C. Ramalho, J. M. Santos, *J. Phys. Chem. A*, **2006**, 110, 1031-1040.

[39] A. Szabo, N. S. Ostlund, Handbook Introduction to Advanced Eletronic Structure Theory. Modern Quantun Chemistry, New York, **1989**.

[40] A. D. Becke, *J. Chem. Phys.*, **1993**, *98*, 1372-1377.

[41] S. G. Lee, Y. C. Chung, *J. Appl. Phys*., **2009**, *105*, 34902-1-34902-4.

[42] M. J. Frisch, J. A. Pople, J. S. Bintley, *J. Chem. Phys*., **1984**, *80*, 3265-3269.

[43] R. Krishnan, T. S. Binkley, R. Seeger, J. A. Pople, *J. Chem. Phys*., **1980**, *72*, 650-654.

[44] E. van Lenthe, E. J. Baerends, J. G. Snijders, *J. Chem. Phys*., **1994**, *101*, 9783-9792.

[45] G. Te Velde, F. M. Bickelhaupt, E. J. Baerends, *J. Comp. Chem*., **2001**, *22*, 931-967.

[46] a) E.J. Baerends, T. Ziegler, J. Autschbach, D. Bashford, A. Bérces, F.M. Bickelhaupt, C. Bo, P.M.Boerrigter, L. Cavallo, D.P. Chong, L. Deng, R.M. Dickson, D.E. Ellis, M. van Faassen, L. Fan, T.H.Fischer, C. Fonseca Guerra, A. Ghysels, A. Giammona, S.J.A. van Gisbergen, A.W. Götz, J.A.Groeneveld, O.V. Gritsenko, M. Grüning, S. Gusarov, F.E. Harris, P. van den Hoek, C.R. Jacob, H.Jacobsen, L. Jensen, J.W. Kaminski, G. van Kessel, F. Kootstra, A. Kovalenko, M.V. Krykunov, E. vanLenthe, D.A. McCormack, A. Michalak, M. Mitoraj, J. Neugebauer, V.P. Nicu, L. Noodleman, V.P.Osinga, S. Patchkovskii, P.H.T. Philipsen, D. Post, C.C. Pye, W. Ravenek, J.I. Rodríguez, P. Ros,P.R.T. Schipper, G. Schreckenbach, J.S. Seldenthuis, M. Seth, J.G. Snijders, M. Solà, M. Swart, D.Swerhone, G. te Velde, P. Vernooijs, L. Versluis, L. Visscher, O. Visser, F. Wang, T.A. Wesolowski,E.M. van Wezenbeek, G. Wiesenekker, S.K. Wolff, T.K. Woo, A.L. Yakovlev, ADF2012.01, SCM: Amsterdam, The Netherlands, **2012**; b) ADF 2007.01, SCM, Amsterdam, The Netherlands, **2007**.

[47] F. A. Hamprecht, A. J. Cohen, D. J. Tozer, N. C. Handy, *J. Chem. Phys*., **1998**, *109*: 6264-6271.

[48] G. Menconi, P. J Wilson, D. J. Tozer, *J. Chem. Phys*., **2004**, *114*, 3958-3967.

[49] R. F. W. Bader, Handbook Atoms in Molecules. A Quantum Theory, Clarendon Press, Oxford, **1990**.

[50] K. Morokuma, *J. Chem. Phys*., **1971**, *55*, 1236–1244.

[51] T. Ziegler, A. Rauk, *T. Chim. Acta*, **1977**, *46*, 1–10.

[52] F. M. Bickelhaupt, E. J. Baerends, Handbook Kohn-Sham density functional theory: Predicting and understanding chemistry. Review Computational Chemistry, **2000**, *15*, 1-6.

[53] K. Fukui, *J. Phys. Chem*., **1970**, *74*, 4161-4163.

[54] S. Maeda, Y. Harabuchi, Y. Ono, T. Taketsugu, *Int. J. Quant. Chem*., **2015**, *115*, 258–269.

[55] L. Zhao, M, von Hopffgarten, D. M. Andrada, G. Frenking, *WIREs Comp. Mol. Sci.*, **2018**, *8*, e1345.

[56] M. von Hopffgarten, G. Frenking, *Wiley Interdiscip. Rev. Comput. Mol. Sci*., **2012**, *2*, 43-62.

[57] L. P. Wolters, F. M. Bickelhaupt, *Chem. Open*, **2012**, *1*, 96-105.

[58] M. A. Spackman, E. N. Maslen, *J. Phys. Chem*., **1986**, *90*, 2020–2027.

[59] D. H. Pereira, F. A. La Porta, R. T. Santiago. D. R. Garcia, T. C. Ramalho, *Revista Virtual da Química*, **2016**, *8*, 425-453.

[60] M. P. Freitas, T. C. Ramalho, In Handbook Princípios de estrutura eletrônica e orbitais em química orgânica – Lavras: Ed. UFLA, **2013**.

[61] D. Balcells, E. Clot, O. Eusnstein, *Chem. Rev*., **2010**, *110*, 749-823.

[62] D. Astruc, *New J. Chem*., **2005**, *29*, 42-56.

[63] E. C. Sherer, C. J. Cramer, *Organometallics*, **2003**, *22*, 1682-1689.

[64] M. Brookhart, M. L. H. Green, G. Parkin, *PNAS*, **2007**, *104*, 6908-6914.